Movement of Overburden Stratum and Damage Evolution of Floor Stratum during Coal Mining above Aquifers

Ruifu Yuan[a,b]*, Yingqiang Li[a], Zhenhua Jiao[a]

aSchool of Energy Science and Engineering, Henan Polytechnic University, Jiaozuo 454003, China
bInstitute of Mechanics, Chinese Academy of Sciences, Beijing 100190, China

Abstract

Based on coal mining above aquifers of Carboniferous limestone in a coal mine in North China Mining Area, the numerical method of CDEM (Continuum-based Discrete Element Method) was employed to simulate the movement of overburden stratum and damage evolution of floor stratum during coal mining above aquifers. The results indicated that the lithology, thickness, and structure of the impermeable strata and the pressure of confined water were the most pivotal elements which lead to the risk of water inrushes and damage evolution of floor stratum. In addition, the activities of overburden stratum, such as deformation, stratum separation, caving, also exhibited important effects. Compared to caving activities of the immediate roof and main roof, the critical upper strata with the larger thickness and strength showed more important influence on the damage evolution of floor stratum and water inrush risk, although it was relatively far from the coal seam. Before the initial caving of critical roof, the destruction extent of floor stratum and the risk of water inrush increased with the increase of the mined-out area and reached their peaks when the maximum caving interval was reached. When critical strata started periodic caving, the extent of destruction of floor and the risk of water inrush reached their peaks when hanging arch of critical strata reached the maximum value in this period. For caving interval in critical strata is larger than the mail roof and the stress pressure was mainly applied in the rear of the mined-out area other than the mining face, it is difficult to observe the rules of the activities of critical strata above coal seam through conventional mining monitoring ways. The activities of critical strata above coal seam should be studied to effectively prevent water inrush disaster in coal mine.

* Corresponding author. Tel.: +0-391-3987931; fax: +0-391-3987937.
E-mail address: yrf@hpu.edu.cn

1. Introduction

Coal mining activities in coal seams of Shanxi Formation in North China are affected by limestone aquifer in the lower Taiyuan Formation. In the mining area with large aquifers, coal mining above aquifers is often required. Under the combination of additional mining stress and the pressure of aquifers, the stability determination of the water-resisting layer of floor stratum is the critical to predict the risk of water inrushes. Although the common determination method[1,2] has been widely used in China, related calculation formula are based on the analytical calculation of elasticity or fitting with empirical data. Moreover, the liquid-solid coupling interaction is not considered in previous calculation formula, which shows some limitations.

The failure mechanism of floor strata and related risk determination basis are always important in the study of water inrush control in coal mining. Baiying Li et al.[3,4] proposed the Theory of "Down Three Zones" of coal bed floor strata above aquifers, which was widely applied to guide coal mining. For mining geological conditions are quite different in various mines and the application scope of single theory or analysis method is often restricted, the theoretical analysis and numerical simulation for water inrush risk based on geological exploration and water level determination are of great practice value in specific mines or mining projects. Qinglong Shi,[5] Xiangrui Meng,[6] Rui Zhang,[7] and Hongfei Duan [8] respectively studied the stress distribution and destruction rule of floor strata after coal mining through the re-analysis and numerical simulation with on-site monitoring data. Yaoqing Hu [9] studied the monitoring and forecasting theory of water inrush during coal mining above aquifers through the combination of numerical simulation and physical monitoring and proposed that water inrush disaster was gradually developed. Therefore, the sensitive information of the development process allows the prediction and control of water inrushes. Jin'an Wang [10] studied the failure rule of floor strata under the combined influences of karst water and Ordovician limestone and believed that only coalbed destruction zone was developed in the initial mining stage and that new damaged zone or mining-induced water conductive zone was mainly formed below the working surface in the full mining stage. Jian Sun [11] successfully predicted water inrush of floor faults through capturing fault activation information with microseismic signals.

During the mining under aquifers, overburden stratum, floor stratum, and high pressure aquifer is interconnected with each other. For the scope and status of overburden stratum caving (deformation) vary with mining stage, floor stratum damage and seepage are also changed in different mining stages. CDEM (Continuum-based Discrete Element Method) numerical simulation proposed by Li et al.[12,13] is the continuum-discrete element method based on the continuum-discrete coupling analysis idea. In the method, before rock rupture, according to continuous finite element calculations, Mohr-Coulomb and maximum composite tensile stress criterion was introduced to judge the rupture state and rupturing direction of elements and to simulate internal and boundary rupture of elements. After rock rupture, the non-continuous discrete element calculation method can be used to simulate the whole process of rock stratum, including deformation, rupture, caving, and compaction. The method provided a new tool to study movement of surrounding strata in coal mines.

In the paper, based on the monitoring data of rock layer and water level, with the numerical simulation method CDEM, we analyzed the rupture of rock layers of floor stratum and stress distribution rule during coal mining under aquifers and revealed the mechanism of water inrushes during coal mining under aquifers.

2. Geological Conditions and Hydraulic Parameter Analysis

2.1. Geological Conditions

The coal mine is located in south central North China Plain and mining the No. 21 coal seam of Shanxi Formation. Hydrogeological conditions in the mine belong to typical North China hydrogeological conditions and are affected by the Cambrian Formation, Ordovician Formation, and the lower limestone aquifers of Taiyuan Formation. In the

mining area, the average vertical interval from the aquifers of Cambrian and Ordovician limestone to the No. 21 coal seam is 80 m. In the vertical interval, aluminum mudstone of Benxi Formation and the impermeable layer of sandstone and mudstone in the medium Taiyuan Formation block the connection between the medium Taiyuan Formation and the lower Taiyuan Formation and show no direct effect on coal mining in the No. 21 coal seam. The confined aquifers (C_2tL_{7-9}) in the upper limestone of Taiyuan Formation of the Upper Carboniferous are composed of 2 to 3 layers of gray and dark limestone, in which the L_{7-8} layer is stable with developed fractures and the No. 21 coal seam is connected with floor stratum aquifers. The aquifer is 10-20 cm away from the No. 21 coal seam and shows medium water enrichment. Water filling form is mainly water gushing from fracture, which shows the great impact on coal mining.

Formation	Depth/m	Thickness/m	Sketch	Serial NO.	lithology
Shanxi Formation				0	21 coal seam
	6.00	6.00		1	mudstone
	6.20	0.20		2	siderite mudstone
	10.20	4.00		3	mudstone
	13.20	3.00		4	limestone(L_8)
	15.00	1.80		5	mudstone
Taiyuan Formation	22.00	7.00		6	limestone(L_7)
	27.00	5.00		7	sandy mudstone
	35.00	8.00		8	packsand
	38.00	3.00		9	sandy mudstone
	44.00	6.00		10	packsand
	46.00	2.00		11	limestone(L_4)
	49.00	3.00		12	mudstone
	62.00	13.00		13	limestone(L_{1-3})
	63.00	1.00		14	11 coal seam
Benxi Formation	64.00	1.00		15	mudstone
	74.00	10.00		16	Aluminum mud

Fig. 1 Aquifers of Taiyuan Formation under No. 21 coal seam

2.2. Analysis of Hydraulic Parameters

In order to grasp the dynamic changes of water levels in C_2tL_{7-8} limestone aquifers, 2 hydrological observation holes were drilled to observe the change in water level. The observation results are shown in Table 1.

Tab. 1 Observation data of water level in L_{7-8} limestone

No.	Ordinates of holes /m			Hole depth/m	Dip angle/°	Flow /m3·h⁻¹	Water pressure/MPa	Monitoring periods
	X	Y	Z					
K1	***4759.9	****0244.4	-9.1	38.0	40	0.45	0.175	16 months
K2	***4774.5	****0015.4	-35.0	43.5	40	1.00	0.50	5 months

The horizontal distance between the two observation holes is 229.5 m and the elevation at hole bottom is 25.9 m. The monitored differential hydraulic pressure is 0.325 MPa. After subtracting differential hydraulic pressure caused by the elevation (0.259 MPa), the hydraulic pressure in deep elevation shows the increasing tendency. According to the vertical depths of the two observation holes, hydraulic pressures applied on floor stratum aquifers at K1 and K2 were respectively 0.42 MPa and 0.78 MPa.

3. Numerical Simulation and Analysis

3.1. Numerical Model

The 2D hexahedral element model was established with finite element software. The model size was 300 m × 100 m. The bottom movement is restricted in the directions of x and y axes. The side movement is restricted in the x direction. The load P is applied on the top to simulate the stratum pressure applied on the No. 21 coal seam (embedded depth of 400 m). Confined aquifer is in the lower section of the No. 21 coal seam. According to the measured data, the thickness of two impermeable layers is respectively selected as 10 m and 19 m. Internal hydraulic pressure of aquifers is Pw, as shown in Figure 2. The stratum sizes and relevant mechanical parameters are shown in Table 2.

After the model is established, equilibrium state was firstly calculated according to the preset boundary conditions. Then, the excavation was performed step by step. Excavation depth in every step was 20 m. After every excavation step, model equilibrium state was calculated. The corresponding relationship between excavation width and calculation step is shown in Table 3. Four monitoring points were arranged on both top and bottom of the impermeable layer (M_1~M_8). Displacement, stress, destruction state, and other data of floor stratum during excavation were recorded.
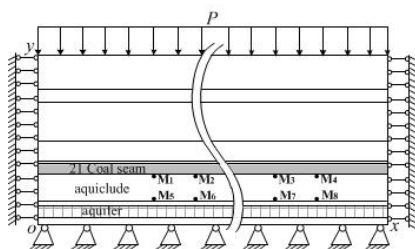

Fig. 2 Numerical model

Tab. 2 Arrangement and mechanical parameter of rock stratum in numerical model

No.	Lithology	Y-axis ordinate /m	Mechanical parameters of elements						Joint mechanical parameters within rock stratum					Joint mechanical parameters among rock stratum				
			Density/(kg·m^{-3})	Elastic modulus /Pa	Poisson's ratio	Cohesion/Pa	Compressive strength/Pa	Friction angle /(°)	Normal stiffness/Pa	Tangential stiffness/Pa	Friction angle /(°)	Cohesion/Pa	Tensile strength/Pa	Normal stiffness/Pa	Tangential stiffness/Pa	Friction angle /(°)	Cohesion/Pa	Tensile strength/Pa
1	Limestone	0~5	2680	17.3e9	0.19	9.3e6	1.9e6	37	5e10	5e10	30	9.3e6	1.9e6	5e10	5e10	20	0	0
2	Limestone	5~14	2610	17.3e9	0.19	9.3e6	1.9e6	37	5e10	5e10	30	9.3e6	1.9e6	5e10	5e10	20	0	0
3	Sandy mudstone	14~17	2660	37.0e9	0.22	17.0e7	2.7e6	28	5e10	5e10	25	17.0e7	2.7e6	5e10	5e10	20	0	0
4	Mudstone	17~36	2410	10.2e9	0.28	2.9e6	0.9e6	35	5e10	5e10	25	2.9e6	0.9e6	5e10	5e10	20	0	0
5	Coalbed	36~43	1411	3.3e9	0.30	1.1e6	0.3e6	26	5e10	5e10	35	1.1e6	0.3e6	5e10	5e10	20	0	0
6	Mudstone	43~45	2350	7.3e9	0.31	0.8e6	0.5e6	33	5e10	5e10	35	0.8e6	0.5e6	5e10	5e10	20	0	0
7	Gritstone	45~59	2622	14.0e9	0.25	5.6e6	0.9e6	27	5e10	5e10	28	5.6e6	0.9e6	5e10	5e10	20	0	0
8	Sandy mudstone	59~86	2566	8.5e9	0.28	3.0e6	0.7e6	34	5e10	5e10	26	3.0e6	0.7e6	5e10	5e10	20	0	0
9	Sandy mudstone	86~96	2547	16.0e9	0.26	3.2e6	1.5e6	34	5e10	5e10	28	3.2e6	1.5e6	5e10	5e10	20	0	0
10	Mudstone	96~	2451	7.1e9	0.29	2.2e6	0.8e6	35	5e10	5e10	35	2.2e6	0.8e6	5e10	5e10	20	0	0

120

Tab. 3 Calculation step vs. excavation width

Excavation ordinates x/m	Excavation width/m	Starting step/10^4	Completion Step/10^4
100~120	20	0	1.4
120~140	40	1.4	8.2
140~160	60	8.2	12.4
160~180	80	12.4	16.2
180~200	100	16.2	20.4
200~220	120	20.4	24.0
220~240	140	24.0	29.6
240~260	160	29.6	33.0
260~280	180	33.0	38.0
280~300	200	38.0	42.6

3.2. Simulation Results

- Movement of Overburden Strata during the Mining Process

Figure 3 shows the caving process of overburden stratum during coal mining process of the No. 21 coal seam. Figure 6 shows the caving process of various excavation widths (20 m, 40 m, 80 m, 100 m, 120 m, and 200 m from top to bottom). The left column shows the caving process of rock stratum model. The middle column shows the displacement map. The right shows the change in vertical stress.

As shown in Figure 3, the discrete element method (CDEM) based on continuum mechanics can be used to simulate the rupture, caving, and accumulation of rock stratum. After the excavation width reached 40 m, mail roof caving did not occur and stress concentration degree of coalbed in the both sides of the mined-out area was increased, therefore leading to relatively large pressure applied on the both sides of floor stratum. The pressure of overburden stratum was not applied on the impermeable layer of floor stratum of the mined-out area. The impermeable layer belongs to the stress-decreasing zone. If the large pressure is applied on the bottom of the impermeable layer, the impermeable layer is prone to rupture to form water inrush. With the increase in excavation width, the mail roof caving occurred when excavation width reached 60 m. In the mining site, initial pressure was induced, but the upper rock stratum did not move. The separation layer was formed between the mail roof and upper rock stratum and stress concentration degree on both sides of the mined-out area continuously increased. Although the collapsed direct roof and mail roof were accumulated in the mined-out area, the applied vertical stress was still small. However, water inrush risk of floor stratum continuously increased.

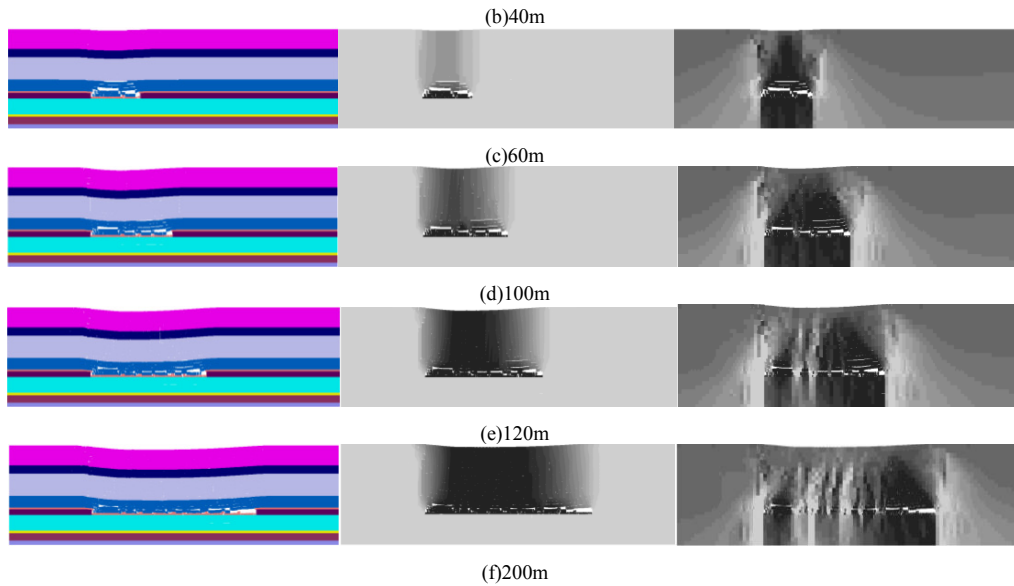(a) 20m

(b)40m

(c)60m

(d)100m

(e)120m

(f)200m
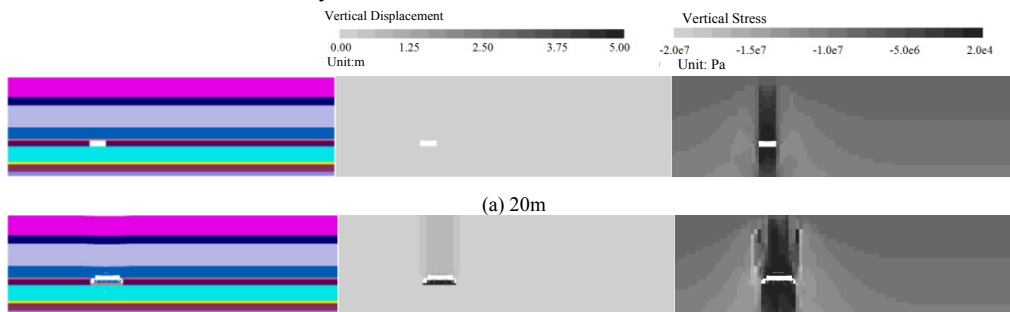
Fig. 3 Movement of overburden stratum and stress distribution during the mining process

As the excavation continued, mail roof began to collapse periodically. When excavation width reached 120 m, the mail roof of the upper critical stratum collapsed and the whole overburden stratum (within the simulation range) began to sink. At this time, floor stratum supported the collapsed rock, thus preventing water inrush in floor stratum. As the excavation continued, the upper critical stratum also entered the periodical caving phase.

- Deformation and Damage Rule of Floor Stratum during the Mining Process

Figure 4 shows the variation of vertical stress at monitoring point which is 5 m below the open-off cut on the floor stratum (coordinates in the model: $x = 95$ m, $y = 31$ m). For the weight of overburden stratum was transferred to both sides after coal mining, the stress at the monitoring point was gradually increased with the increase in the mining scope. In the initial 60-m excavation width, the stress increased firstly and then slowly decreased to a certain value, indicating that rock stratum withstood the larger stress and was prone to deform. After the excavation width reached 80 m, the stress change trend was not significant, indicating that rock stratum reached its strength limit. Under the constraint of surrounding rock, the rock stratum could still withstand the continuously increased stress.

When the excavation width reached 120 m, the stress reached its peak, indicating that the whole stratum (within the model range) started caving. When the excavation width reached 160 m, the stress began to decrease, indicating that the overburden strata collapsed and then pressurized the mined-out area and that waste rock began to bear the weight of the overburden stratum. In the mining site under aquifers, when the stress at the monitoring point in Figure 4 reached its maximum value, coal columns on both sides of the mined-out area led to the most serious damage of floor stratum and the upper impermeable layer within the excavation width withstood no weight or withstood only the weight of rock caving from direct roof and mail roof. Therefore, the upper impermeable layer within the excavation width was easily ruptured.
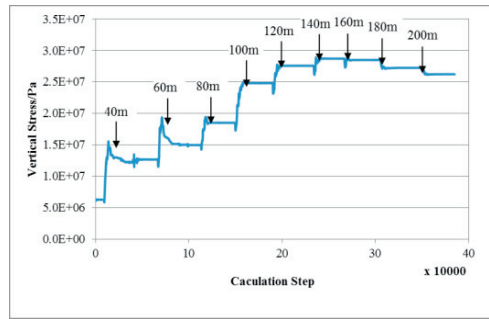
Fig. 4 Vertical stress vs. excavation width at the open-off cut of floor stratum

After coal mining, under the action of concentrated stress on both sides, floor stratum damage occurred. Moreover, the upper floor stratum of the mined-out area lost its constraints and intensified the development of floor fractures under the role of confined water.

Figure 5 shows the fracture distribution of floor stratum and roof stratum of coal seam under different conditions. Without hydraulic pressure (Pw=0 MPa), floor stratum fractures were only caused by stress change of surrounding strata and the formed fractures were mainly the interformational fractures. Intraformational fractures were formed in the utmost upper floor stratum and the fracture density is small (Figure 5(a)). Under the action of hydraulic pressure, when the thickness of the impermeable layer of floor stratum was large (19 m), hydraulic pressure showed small damaging effect on floor stratum and fracture distribution showed no significant change (Figures 5(a) and 5(b)). When the thickness of the impermeable layer of floor stratum was small (10 m), the role of hydraulic pressure was significant. Under the same stress, hydraulic pressure increased displacement and damage of floor stratum. More intraformational and interformational fractures were developed in the floor stratum (Figure 5(c)).

Figure 6 is the displacement contour map of the 10-m thick impermeable layer under the mining conditions under aquifers. Under the role of hydraulic pressure, macro fractures were formed between the aquifer and the impermeable layer. When excavation width reached 60 m (Figure 6(a)), mail roof did not completely collapse. For the upper impermeable layer was the free layer, the stress concentrated on both sides together with hydraulic pressure lifted the floor stratum, thus leading to macro fractures. With the increase of excavation width, fracture length and width were increased. When excavation width reached 100 m (Figure 6(b)), although the mail roof collapsed, the upper critical stratum did not rupture, leading to the increasing fractures and the increasing risk of water inrush. When excavation width reached 120 m, the upper critical stratum ruptured and the floor stratum in the mined-out area was re-compacted. Therefore, previously formed macro fractures were closed and became small. In the rear of mining surface, roof stratum was still hanging and did not collapse completely and fractures still existed. After the advancement of mining surface, the influencing area was 60 m away from the rear of the working surface. The influencing area was also the critical region for the control of water inrush (Figures 6(c) and 6(d)).
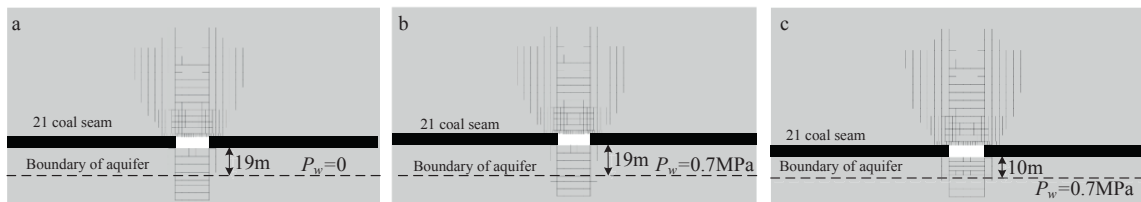

Fig. 5 Fracture distribution in surrounding rock stratum under different geological conditions. (a) The 19 m thick impermeable layer without hydraulic pressure; (b) The 19 m thick impermeable layer with hydraulic pressure; (c) The 19 m thick impermeable layer with hydraulic pressure.
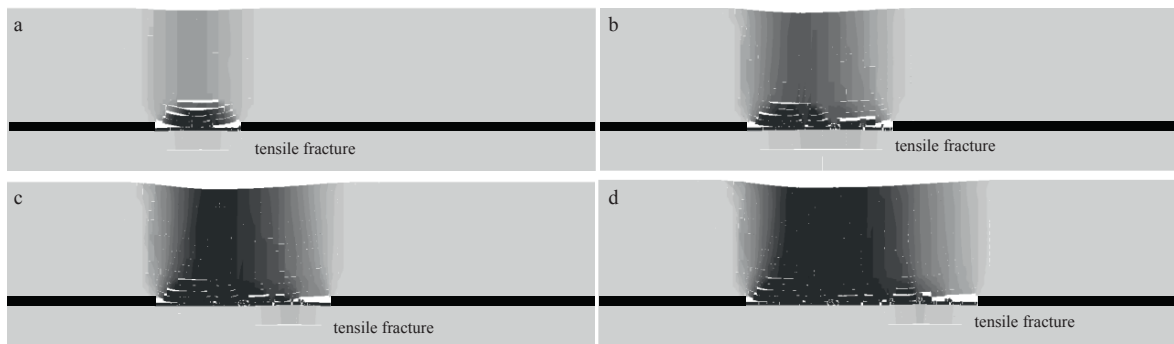
Fig. 6 Evolution of main fracture in the floor stratum in the process of excavation when the aquifer is 10 m thick. (a)Excavation width of 60 m (b) Excavation width of 100 m(c) Excavation width of 120 m (d) Excavation width of 160 m

Figure 7 shows the displacement variation of the monitoring point on the 110-m excavation width in the floor stratum under three situations (model coordinates: x = 210 m, y = 36 m). The calculation step of the horizontal coordinates corresponding to excavation width can be found in Table 3.

In the early excavation stage, for the monitoring point was far from the influencing area, the displacement was relatively small. When the excavation width reached 80 m, the influence on the monitoring point was increased and the monitoring point showed the stepped decline, which corresponded to the stepped increase of the stress on the rock on both sides of the mined-out area, as shown in Figure 4. When coal seam at the monitoring point was excavated, the displacement of the monitoring point was rapidly fluctuating upward and the displacement reached 10-20 cm within short term. The rapid short-term displacement is very unfavorable to water inrush prevention. Figure 7 shows the comparison results of the displacement changes obtained the case with hydraulic pressure and the case without hydraulic pressure. When the impermeable layer was 19 m thick, the confined aquifer showed relatively small effects on displacement change and final displacement. When the impermeable layer was 10 m thick, the effects of the confined aquifer on displacement change and final displacement reached 50%. Especially, when short-term displacement was fluctuating, the hydraulic pressure significantly increased the upward displacement of floor stratum. Therefore, the rupture risk of floor stratum was significantly increased.

As the excavation continued, overburden stratum completely collapsed and then pressurized floor stratum. Surrounding stratum became stable and the displacement of the monitoring point was not changed.
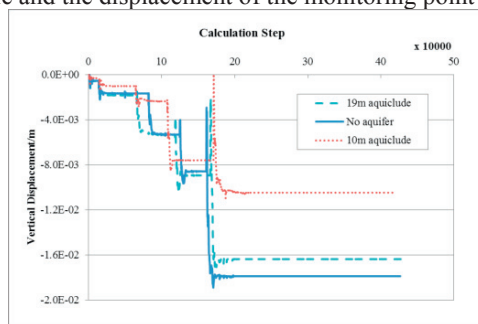

Fig. 7 Displacement variation of the point on the 110-m excavation width in the floor stratum

4. Discussion of the risks of overburden stratum caving and water inrush

Obviously, lithology, thickness, structure parameters, and hydraulic pressure of confined water of the impermeable layer are the critical factors in determining the risk of water inrush. Under the constant conditions of

the above factors, coal mining technologies and the activities of overburden strata show an important impact on water inrush risk and the damage extent of floor stratum. Floor deformation and damage caused by coal mining are the dynamic processes. The deformation and destruction of floor stratum vary with mining method, mining area and caving state of overburden stratum. During mining under aquifers, risk evaluation and control of water inrushes of floor stratum should be adapted to the dynamic mining process.

Coal mining advancement started from the open-off cut. With the increase in the mining area, mining site respectively experienced the initial water pressure conduction stage and periodical conduction stage, which respectively corresponded to the initial caving and periodical caving of mail roof. For the caving rate of the upper rock stratum which was far from mining site lagged behind the advancement rate, hydraulic pressure change caused by caving was far from mining site. Therefore, the pressure change in mining site was not significant. However, the caving showed important effects on the pressure change of floor stratum in the mined-out area and stress concentration area of coal seam, which affected water inrush risk of mining under aquifers.

Water inrush risk is closely related to the thickness, lithology, and integrity of the impermeable layer of floor stratum as well as roof structure. When roof stratum contained much soft rock, if caving interval of rock stratum was short, stress concentration degree on both sides of the mined-out area was low. Therefore, the impermeable layer of floor stratum could be timely compacted by the caving rock to prevent the control of water inrushes. If roof stratum or the lower rock stratum which was close to coal seam contained much hard and thick rock stratum, the caving interval was large and the stress on both sides of the mined-out area was often concentrated, thus intensifying the rupture of floor stratum. At the same time, the large-area internal floor stratum in the mined-out area lost constraints and was prone to lead to water inrush accident.

5. Conclusions

(1) The discrete element method (CDEM) based on continuum mechanics can be used to simulate the destruction, caving, and accumulation process of rock stratum. It is a powerful tool to study mining pressure and overburden strata movement.

(2) The step distance of initial conduction of hydraulic pressure was 60 m. The caving step distance of the critical rock stratum was 120 m. Before the caving of the critical stratum, the stress concentration degree in the mined-out area continuously increased with the increase of the mining area. The non-constrained roof area of floor stratum continuously increased. Therefore, floor stratum showed the maximum damage degree when excavation width reached 120 m.

(3) After the critical stratum experienced the initial caving, it gradually entered the stage of periodic caving. The caving step was about 60 m, which was more than initial water head of mail roof. Therefore, during the 60-m advancement, the floor strata withstood the larger hydraulic pressure.

(4) The lithology, thickness, and structure of the impermeable layer of floor stratum as well as hydraulic pressure of confined aquifers are the most important factors of water inrush risk. When the impermeable layer was 19 m thick, C_2L_{7-8} aquifer showed less effect on deformation and damage of the impermeable layer, indicating the low water inrush risk. When the impermeable layer was 10 m thick, C_2L_{7-8} aquifer showed significant effect on deformation and damage of the impermeable layer and macro fractures occurred in the impermeable layer of floor stratum, thus increasing water inrush risk. The sizes of macro fractures are related to the caving of critical roof stratum. Therefore, during mining under aquifers, in addition to monitoring hydraulic pressure, it is necessary to analyze and observe the thickness variation of the impermeable layer of floor stratum and movement of overburden stratum.

References

［1］ State Administration of Work Safety, State Administration of Coal Mine Safety. Regulations of prevention and control of water disaster in coal mine[S]. Beijing: China Coal Industry Publishing House, 2009.11.(in Chinese)

［2］ Meng Zhaoping, Gao Yanfa, Lu Aihong. Theory and Method of Water Inrush Risk Assessment in Coal Mine. Beijing: Science Press, 2011.6.(in Chinese)

［3］ Li Baiying, Shen Guanghan, Jing Zigang. Theory and practice of prevent water inrush from floor in mining face. Safety In Coal Mines, 1988.05:47~48.(in Chinese)

［4］ Li Baiying. "Down Three Zones" in the Prediction of the water inrush from Coalbed Floor Aquifer-theory，Development and Application [J]. Journal of Shandong University of Science & Technology(Natural Sciences), 1999,18(4):11-18.(in Chinese)

［5］ SHI Long-qing,XU Dong-jing, QIU Mei. Improved on the formula about the depth of damaged floor in working area[J]. Journal of China Coal Society, 2013,38(s2):299-303.(in Chinese)

［6］ MENG Xiangrui, XU Chenghui, GAO Zhaoning, etal. Stress distribution and damage mechanism of mining floor [J]. Journal of China Coal Society, 2010, 35 (11): 1832-1836.(in Chinese)

［7］ ZHANG Rui1,JIANG Zhen-quan,LI Xiu-han et al. Study on the failure depth of thick seam floor in deep mining [J]. Journal of China Coal Society, 2013,38(1):67-72.(in Chinese)

［8］ DUAN Hongfei,JIANG Zhenquan,ZHANG Rui, et al. Field measurement and simulation research on failure depth of fully mechanized thin coal seam floor in Yangcun Coal Mine [J]. Journal of China Coal Society, 2011,36(s1):13-17.(in Chinese)

［9］ HU Yaoqing，YAN Guochao，SHI Xiuwei. Study on physical and numerical simulation of water inrush prediction theory for coal mining above confined aquifer[J]. Chinese Journal of Rock Mechanics and Engineering, 2008, 27(1):9~15.(in Chinese)

［10］ WANG Jin-an,WEI Xian-hao,JI Hong-guang. Rupture and seepage law of roof-floor strata caused by coal mining between double-bearing aquifers [J]. Journal of China Coal Society, 2012,37(6):891-897.(in Chinese)

［11］ SUN Jian, WANG Lian-guo. Floor fault water-inrush prediction based on catastrophe analysis of micro-seismic signals [J]. Journal of China Coal Society, 2013,38(8):1404-1410.(in Chinese)

［12］ Li S H, Zhang Y N, Feng C. A spring system equivalent to continuum model. In: The Fifth International Conference on Discrete Element Methods, London, 2010. 75－85.

［13］ Feng C, Li S H, Yao Z X. Study of block-discrete-spring method based on continuum mechanics[J]. Chin J Rock Mech Eng, 2010,29(S1): 2690－2704.(in Chinese)